

ChemComm

Accepted Manuscript



This is an *Accepted Manuscript*, which has been through the Royal Society of Chemistry peer review process and has been accepted for publication.

Accepted Manuscripts are published online shortly after acceptance, before technical editing, formatting and proof reading. Using this free service, authors can make their results available to the community, in citable form, before we publish the edited article. We will replace this *Accepted Manuscript* with the edited and formatted *Advance Article* as soon as it is available.

You can find more information about *Accepted Manuscripts* in the [Information for Authors](#).

Please note that technical editing may introduce minor changes to the text and/or graphics, which may alter content. The journal's standard [Terms & Conditions](#) and the [Ethical guidelines](#) still apply. In no event shall the Royal Society of Chemistry be held responsible for any errors or omissions in this *Accepted Manuscript* or any consequences arising from the use of any information it contains.

Cite this: DOI: 10.1039/c0xx00000x

www.rsc.org/xxxxxx

ARTICLE TYPE

Brominated Single Walled Carbon Nanotubes as Versatile Precursors for Covalent Sidewall Functionalization

Ferdinand Hof,^a Frank Hauke^a and Andreas Hirsch^{*a}

Received (in XXX, XXX) Xth XXXXXXXXX 20XX, Accepted Xth XXXXXXXXX 20XX

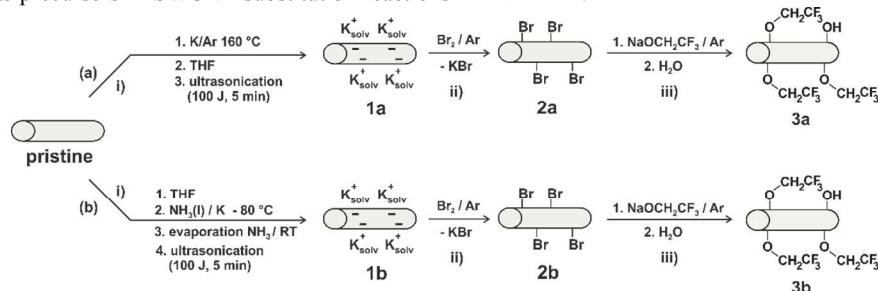
DOI: 10.1039/b000000x

Herein we report on the facile preparation of brominated SWCNTs based on two complementary reductive activation routes. The respective brominated SWCNTs are highly reactive and can be used in nucleophilic substitution reactions and represent versatile starting materials for the generation of sidewall functionalized SWCNTs with a high density of functional moieties.

Throughout the last decade, single walled carbon nanotube (SWCNT) chemistry has gained a lot of interest with respect to covalent framework functionalization and functional group conversion.^{1, 2} In this context, remarkable progress has been made, both in the sense of the exploration of the chemical reactivity of SWCNTs³⁻⁶ as well as in terms of the analytical product characterization.^{7, 8} Nevertheless, the establishment of highly functional organic moieties, covalently connected with the carbon nanotube framework, still remains challenging and is primarily based on stepwise reaction pathways, utilizing carbon nanotube derivatives with covalently attached anchor groups, e.g. hydroxyl functionalities.⁹ Due to the low intrinsic reactivity of SWCNTs relative harsh reaction conditions are needed for covalent framework addition reactions. As a consequence successfully attached functional entities are limited to carboxyl groups^{10, 11}, phenyl^{12, 13} or alkyl addends¹⁴ or hydroxy functionalities.¹⁵ In contrast to addition reactions, nucleophilic SWCNT substitution reactions have hardly been investigated and are solely based on fluorinated carbon nanotube precursors.¹⁶⁻¹⁸ For instance, Stevens *et al.* have shown that fluorine substituents on SWCNTs can be substituted by alkyl groups from Grignard and alkyllithium reagents.¹⁹ The main disadvantage of fluorinated carbon nanotubes as precursors in SWCNT substitution reactions

are their relatively harsh formation conditions, which do not allow to easily control the degree of addition. In principle other halogenated carbon nanotubes, like brominated^{20, 21} or iodinated²² SWCNTs are also accessible, but these systems have not been used for subsequent derivatization reactions.

Here, we report on the synthesis and unambiguous characterization of brominated SWCNTs in combination with a subsequent nucleophilic substitution approach (Scheme 1). Key step of this straightforward synthetic approach was the usage of reduced carbon nanotubides SWCNT^{tr-} as highly reactive intermediates. The reductive activation of the SWCNT (HiPco) starting material was achieved by two different approaches: (a) molten potassium metal based reduction, leading to the formation of the species **1a**⁵ or (b) Birch type reduction^{12, 14, 23} with potassium dissolved in liquid ammonia, yielding species **1b**.¹² This initial reduction step is a fundamental prerequisite which leads to an efficient SWCNT individualization and charged induced reactivity increase for the subsequent bromine addition. The respective brominated SWCNTs **2a**, **2b** represent highly reactive species. We have found that the addition of water leads to an efficient nucleophilic substitution of the covalently bound sidewall bromine atoms and to the formation of hydroxylated SWCNT derivatives. Because of this pronounced reactivity the detailed Raman spectroscopic characterization of the brominated SWCNTs **2a**, **2b** has been carried out under inert gas conditions, following a procedure that we have recently published.⁵ In order to gain a statistically significant bulk information about the success of the covalent functionalization of the reductively activated SWCNT intermediates **2a**, **2b** with bromine, Scanning Raman Microscopy (SRM) was applied and the respective $I_{(D/G)}$ (intensity ratios of the D- and G-bands) values of the recorded



Scheme 1: Sidewall alkoxide functionalization of SWCNTs *via* i) reduction with molten potassium (pathway a) or Birch type reduction (pathway b) to the corresponding carbon nanotubides **1a** and **1b** followed by ii) bromination to the synthetic precursor building blocks **2a** and **2b** and iii) subsequent nucleophilic substitution with NaOCH₂CF₃ yielding alkoxides **3a** and **3b**, respectively.

Cite this: DOI: 10.1039/c0xx00000x

www.rsc.org/xxxxxx

ARTICLE TYPE

625 individual Raman were plotted as a distribution function (Figure 1).

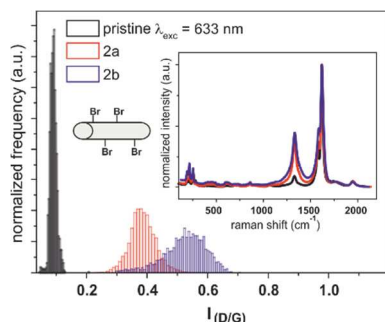
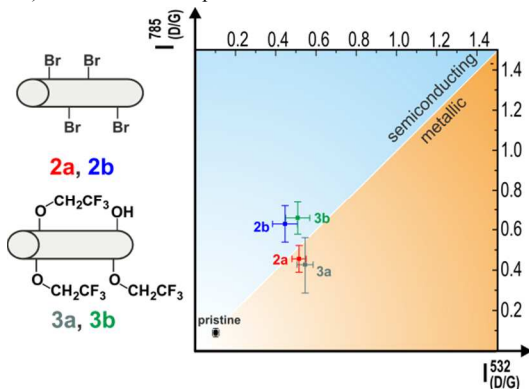


Figure 1: a) Statistical Raman analysis of the brominated SWCNTs adducts **2a** and **2b**; $\lambda_{\text{exc}} = 633$ nm. b) Inset: median spectra.

In general the D-band intensity is a measure of the amount of sp^3 -defects introduced by covalent addend binding. As it can be clearly seen from Figure 1, sidewall brominated SWCNTs are accessible by both reaction pathways, with a mean $I_{(D/G)}$ ratio of about 0.5 by the solid state reduction with potassium and 0.4 in the case of Birch type reduction. The corresponding distribution functions for $\lambda_{\text{exc}} = 532$ nm and $\lambda_{\text{exc}} = 785$ nm are depicted in Figure S1. Using additional excitation energies and organizing the measured data in a 2D-diagram (Figure 2) provides valuable information about the homogeneity distribution (Raman Homogeneity Index (RHI)) and the electronic type selectivity (Raman Selectivity Index (RSI)) of the initial addition reaction (see also Table T1 - ESI).⁸

Figure 2: a) 2-D Raman index plot based on the statistical Raman analysis

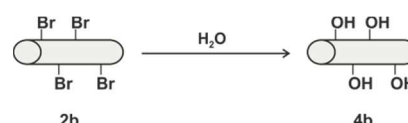


of the samples **2a**, **2b**, **3a**, **3b** at $\lambda_{\text{exc}} = 532$ nm and $\lambda_{\text{exc}} = 785$ nm – for detailed data see Table T1 - ESI.

In contrast to pathway (a), where no selectivity is observed (RSI = 1.9°), the Birch type based addition sequence (b) exhibits a RSI value of 12.3°, indicative for a selectivity in respect to semiconducting SWCNTs. This kind of electronic type selectivity has also been observed with other Birch type based functionalization sequences.¹¹ The Raman based analysis provides a direct insight into the introduction of sp^3 -defects, but does not lead to any information about the chemical nature of the

bound addends. For this purpose, the brominated SWCNT derivative **2b** was analysed by means of thermogravimetric analysis coupled to mass spectrometry (TG/MS) – (Figure 3 – left). Here, a sharp mass loss ($\Delta\text{wt} = 71$ % - corrected by mass loss of pristine starting material – ESI Figure S3) is detected in the region between 250 and 350 °C and can be traced back to the detachment of bromine with the mass fragments m/z 79, 81 (m/z 80, 82 [HBr]) based on its characteristic isotopic distribution (1:1). For **2b**, a degree of functionalization of about 5 % can be calculated. The covalently bound bromine addends can easily and quantitatively be substituted by the addition of water (Scheme 2).

Scheme 2: Hydrolysis of brominated SWCNT intermediates, yielding



sidewall hydroxylated SWCNT derivatives **4b**.

This reaction sequence provides a fast access route to hydroxylated SWCNT derivatives **4b**. The detached bromide ions were identified in the aqueous phase by precipitating as silver bromide. The TG/MS analysis of **4b** (Figure 3 – right) corroborated the substitution of the bromo addends. The introduced hydroxyl groups can be identified by their mass fragments m/z 17, 18 (further mass traces see Figures S4) and a sample mass loss of about 8% (after correction – see Figure S3) is detected – no remaining bromine was found for **4b**. Based on this data, the degree of functionalization before and after hydrolysis is determined as about 5 % and remains practically unchanged which is indicative for a quantitative substitution of the bromine atoms.

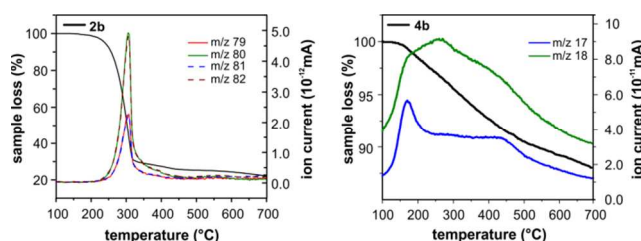


Figure 3: TG/MS profiles of brominated SWCNTs **2b** (left) and hydroxylated SWCNTs **4b** (right).

Hydroxylated carbon nanotubes **4b** may serve as highly functionalized starting materials in subsequent coupling reactions with carboxylic acid derivatives, alternatively, the functional entity can directly be brought in by the reaction of brominated SWCNTs with functional alcohols. The feasibility of this concept has been exemplarily proven by the reaction of **2a** and **2b** with 2,2,2-trifluoro ethanolate (Scheme 1). The trifluoro ethanol group serves as a suitable marker for the TG/MS analysis (Figure 4). In the main mass loss region (100 – 400 °C, 9 % corrected mass loss) all characteristic mass fragments of the trifluoro

ethanol group were detected: m/z 69 $-CF_3$, m/z 70 HCF_3 , m/z 99 F_3CCH_2O- , m/z 100 F_3CCH_2OH . Again, in both substitution products **3a** and **3b** no traces of bromine were detected by TG/MS, indicative for a quantitative substitution of the initially bound bromo addends.

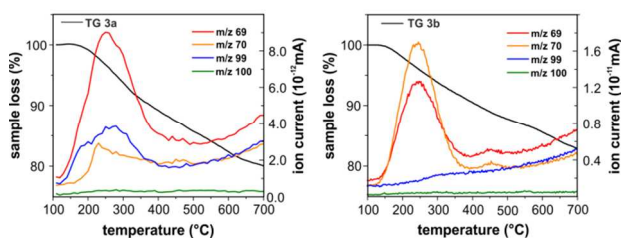


Figure 4. TG/MS profiles of final substitution products **3a** (left) and **3b** (right).

This fact is furthermore corroborated by statistical Raman analysis of the final substitution products **3a** and **3b**. Here, it can be shown that the initial density of defects, present in the respective brominated SWCNT derivatives **2a** and **2b**, is virtually not increased after the addition of 2,2,2-trifluoro ethanolate (Figure 2). Therefore, no additional carbon lattice sp^3 centers are introduced during this part of the functionalization sequence. Moreover, as clearly can be seen by the 2D-Raman index plot, the initial electronic type discrimination with respect to semiconducting SWCNT species (represented by the RSI values – Table T1) remains unchanged by the subsequent substitution reaction. In a reference experiment we have also investigated whether the observed data can be traced back to a direct nucleophilic sidewall addition of 2,2,2-trifluoro ethanolate (Scheme S1). Therefore, pristine HiPco SWCNTs were reacted with the alcoholate under the same reaction conditions as used for the bromo substitution sequence. The respective Raman spectra and TG/MS data (Figure S5) unequivocally show that an attachment of 2,2,2-trifluoro ethanolate does not take place. This clearly demonstrates that a nucleophilic substitution mechanism of brominated SWCNTs is responsible for the formation of the alkoxytated tubes **3a**, **3b**.

Conclusions

Brominated carbon nanotubes, accessible by a direct reductive bromination sequence, serve as versatile building blocks for the facile generation of sidewall functionalized SWCNT derivatives. Two complementary routes were used for the synthesis of these highly reactive intermediates: (a) solid state reduction of SWCNTs with potassium and (b) Birch type reduction with subsequent reaction with bromine, respectively. The bromo addends are easily and quantitatively substituted by water or alcoholates *via* a nucleophilic substitution pathway. This process does not lead to an additional introduction of framework sp^3 centers, which is confirmed by Scanning Raman Microscopy (SRM). In the case of the Birch type reduction sequence, an electronic type selective framework functionalization with respect to semiconducting species is observed. Based on their easy access and high reactivity brominated SWCNTs can serve as a versatile starting material for the generation of multifunctional SWCNT architectures for future applications. Research with respect to this goal is currently pursued in our laboratory.

Notes and references

^a Department of Chemistry and Pharmacy and Institute of Advanced Materials and Processes (ZMP), Friedrich-Alexander-Universität Erlangen-Nürnberg (FAU), Henkestrasse 42, 91054 Erlangen (Germany) Fax: 00499131-8526864 Tel: 00499131-8522537
E-mail: mailto:andreas.hirsch@fau.de

† Electronic Supplementary Information (ESI) available: Experimental details regarding the synthesis of the different SWCNTs derivatives, additional Raman analysis and TG/MS data. See DOI: 10.1039/b000000x/
The authors thank the Deutsche Forschungsgemeinschaft (DFG - SFB 953, Project A1 “Synthetic Carbon Allotropes”) and the Interdisciplinary Center for Molecular Materials (ICMM) for the financial support.

- S. A. Hodge, M. K. Bayazit, K. S. Coleman and M. S. P. Shaffer, *Chem. Soc. Rev.*, 2012, **41**, 4409-4429.
- V. Georgakilas, K. Kordatos, M. Prato, D. M. Guldi, M. Holzinger and A. Hirsch, *J. Am. Chem. Soc.*, 2002, **124**, 760-761.
- Z. Syrgiannis, V. La Parola, C. Hadad, M. Lucío, E. Vázquez, F. Giacalone and M. Prato, *Angew. Chem. Int. Ed.*, 2013, **52**, 6480-6483.
- B. Vanhorenbeke, C. Vriamont, F. Pennetreau, M. Devillers, O. Riant and S. Hermans, *Chem. Eur. J.*, 2013, **19**, 852-856.
- F. Hof, S. Bosch, S. Eigler, F. Hauke and A. Hirsch, *J. Am. Chem. Soc.*, 2013, **135**, 18385-18395.
- C. Zhao, Y. Song, K. Qu, J. Ren and X. Qu, *Chem. Mater.*, 2010, **22**, 5718-5724.
- M. S. Dresselhaus, A. Jorio, M. Hofmann, G. Dresselhaus and R. Saito, *Nano Lett.*, 2010, **10**, 751-758.
- F. Hof, S. Bosch, J. M. Englert, F. Hauke and A. Hirsch, *Angew. Chem. Int. Ed.*, 2012, **51**, 11727-11730.
- T. Palacin, H. L. Khanh, B. Jousset, P. Jegou, A. Filoramo, C. Ehli, D. M. Guldi and S. Campidelli, *J. Am. Chem. Soc.*, 2009, **131**, 15394-15402.
- H. Yu, Y. Jin, F. Peng, H. Wang and J. Yang, *J. Phys. Chem. C*, 2008, **112**, 6758-6763.
- B. Gebhardt, F. Hof, C. Backes, M. Müller, T. Plocke, J. Maultzsch, C. Thomsen, F. Hauke and A. Hirsch, *J. Am. Chem. Soc.*, 2011, **133**, 19459-19473.
- Y. Ying, R. K. Saini, F. Liang, A. K. Sadana and W. E. Billups, *Org. Lett.*, 2003, **5**, 1471-1473.
- C. A. Dyke and J. M. Tour, *J. Phys. Chem. A*, 2004, **108**, 11151-11159.
- F. Liang, A. K. Sadana, A. Peera, J. Chattopadhyay, Z. Gu, R. H. Hauge and W. E. Billups, *Nano Lett.*, 2004, **4**, 1257-1260.
- B. Gebhardt, Z. Syrgiannis, C. Backes, R. Graupner, F. Hauke and A. Hirsch, *J. Am. Chem. Soc.*, 2011, **133**, 7985-7995.
- L. Valentini, J. Macan, I. Armentano, F. Mengoni and J. M. Kenny, *Carbon*, 2006, **44**, 2196-2201.
- L. Zhang, V. U. Kiny, H. Peng, J. Zhu, R. F. M. Lobo, J. L. Margrave and V. N. Khabashesku, *Chem. Mater.*, 2004, **16**, 2055-2061.
- M. X. Pulikkathara, O. V. Kuznetsov and V. N. Khabashesku, *Chem. Mater.*, 2008, **20**, 2685-2695.
- J. L. Stevens, A. Y. Huang, H. Peng, I. W. Chiang, V. N. Khabashesku and J. L. Margrave, *Nano Lett.*, 2003, **3**, 331-336.
- J. F. Colomer, R. Marega, H. Traboulsi, M. Meneghetti, G. Van Tendeloo and D. Bonifazi, *Chem. Mater.*, 2009, **21**, 4747-4749.
- W. Z. Wang, A. S. Mahasin, P. Q. Gao, K. H. Lim and M. B. Chan-Park, *J. Phys. Chem. C*, 2012, **116**, 23027-23035.
- K. S. Coleman, A. K. Chakraborty, S. R. Bailey, J. Sloan and M. Alexander, *Chem. Mater.*, 2007, **19**, 1076-1081.
- J. Chattopadhyay, S. Chakraborty, A. Mukherjee, R. Wang, P. S. Engel and W. E. Billups, *J. Phys. Chem. C*, 2007, **111**, 17928-17932.